Elastic Properties of 4–6 nm-thick Glassy Carbon Thin Films

M. P. Manoharan · H. Lee · R. Rajagopalan · H. C. Foley · M. A. Haque

Abstract Glassy carbon is a disordered, nanoporous form of carbon with superior thermal and chemical stability in extreme environments. Freestanding glassy carbon specimens with 4–6 nm thickness and 0.5 nm average pore size were synthesized and fabricated from polyfurfuryl alcohol precursors. Elastic properties of the specimens were measured in situ inside a scanning electron microscope using a custom-built micro-electro-mechanical system. The Young's modulus, fracture stress and strain values were measured to be about 62 GPa, 870 MPa and 1.3%, respectively; showing strong size effects compared to a modulus value of 30 GPa at the bulk scale. This size effect is explained on the basis of the increased significance of surface elastic properties at the nanometer length-scale.

Keywords Young's modulus · Glassy carbon · Thin film · Size effect

Introduction

Nanoporous glassy carbon derived from pyrolysis of the polymer precursor polyfurfuryl alcohol (PFA) is a non-graphitizing carbon [1] that can act as a molecular sieve and has potential applications in catalysis [2] and air separation [3]. Bulk glassy carbon has been commercially used as an electrode material for over half a century due to its excellent thermal stability and resistance to chemical attacks. These properties also make it more suitable than zeolite molecular sieves for applications such as catalyst supports and as selective adsorbents in high temperature [4] and corrosive environments [1]. Its thermal stability has led researchers to suggest it as a possible material for capture and sequestration of carbon dioxide from industrial processes [5]. Its good electrical conductivity lends to applications in microbatteries where micromachined structures of glassy carbon are used as electrodes [6]. Pyrolysis of PFA results in a highly disordered structure, giving rise to porosity, with a pore width in the range of 0.4–0.5 nm [7]. The resultant material has regions of crystalline order, which are typically of short range and on a global scale it can best be described as amorphous. The disorder also causes the material to be non-graphitizing and resists transformation to long-range graphitic structures even at temperatures as high as 2,000 °C [1]. Such non-graphitic nature of PFA-derived glassy carbon has been attributed to the extensively cross-linked structure of the polymer precursor, which results in a kinetically frozen disorder due to a chaotic misalignment of defective graphene sheets [8] upon pyrolysis.

Due to their unique application potentials, the thermophysical properties of glassy carbon have been extensively studied in the literature but only in their bulk form [9–11]. However, nanoporous glassy carbon can also be synthesized in the form of thin films with few nanometers thickness by choosing an appropriate concentration of the polymer precursor (PFA). Such ultrathin films are expected

M. P. Manoharan · M. A. Haque (✉)
Department of Mechanical & Nuclear Engineering,
The Pennsylvania State University, University Park,
PA 16802, USA
e-mail: mah37@psu.edu

H. Lee · R. Rajagopalan
Materials Research Institute, The Pennsylvania State University,
University Park, PA 16802, USA

H. C. Foley
Department of Chemical Engineering, The Pennsylvania State
University, University Park, PA 16802, USA

to exhibit pronounced size effects on their physical properties, yet only a few studies are available for micro [12] and nanoscale [13] glassy carbon structures, with the smallest size around 150 nm. This is because at the 1–5 nm length-scales, even specimen fabrication, manipulation, gripping and alignment required to achieve the desired boundary conditions for mechanical testing are challenging, not to mention the stringent resolution requirement on force and displacement application and measurement. While no such study exists for glassy carbon at this length-scale, the literature contains a few investigations on the mechanical properties of single [14] and multilayer [15] graphitic carbon (graphene) films. These studies use nano-indentation and atomic force microscope (AFM) tip-based three-point bending, respectively. Both these techniques are popular tools used by researchers to measure the Young's modulus of nanoscale materials. However, nano-indentation on such ultrathin specimens requires complex data de-convolution [16–18]. It also introduces highly localized deformation that may not be representative of the entire specimen [19]. AFM tip-based three-point bending requires an extensive understanding of the tip-thin film interaction for accurate and reliable experimental studies. For example, friction (due to slipping) and van der Waals forces between the thin film and tip will introduce errors in measurement of mechanical properties. The influence of these surface forces on the mechanical properties have been shown to be very significant in case of small diameter nanowires (<30–40 nm) [20] and can be expected to have the same effects while measuring the elastic properties of ultrathin films. Also, in the above experiments a fixed–

fixed beam boundary condition was assumed, even though only van der Waal's forces were used to provide the gripping on the substrate.

Experimental Setup

In this study, we use uniaxial tensile testing to measure the elastic properties of a material under uniform deformation. The technique is relatively straightforward as no assumptions or complicated models are needed to measure the Young's modulus, fracture stress and strain. We designed and fabricated a micro-electro-mechanical device to apply uniaxial tensile stresses on the freestanding thin film specimen. Figure 1a shows the device design, where the specimen is mounted between a flexure beam force sensor and a set of 1°-inclined thermal actuator beams. The beams are micromachined from heavily doped (0.001–0.005 Ω-cm) silicon-on-insulator wafers. The thermal actuator beams expand due to Joule heating upon application of a DC voltage, which loads both the specimen and the force sensing beam. The force on the specimen can be obtained from the force equilibrium diagram shown in Fig. 1b. For example, if the stiffness values of the force sensor and the specimen are k_{fs} and k_{sp}, respectively, then the elongation and force in the specimen are given by,

$$\delta_{\text{specimen}} = \delta_1 - \delta_2; \; F_{\text{specimen}} = k_{fs}\delta_2 = \left(\frac{24\kappa}{L_{fs}^3}\right)\delta_2 \qquad (1)$$

where δ_1 and δ_2 are displacements in the thermal actuator and force sensing beams, respectively, and κ is the in-plane
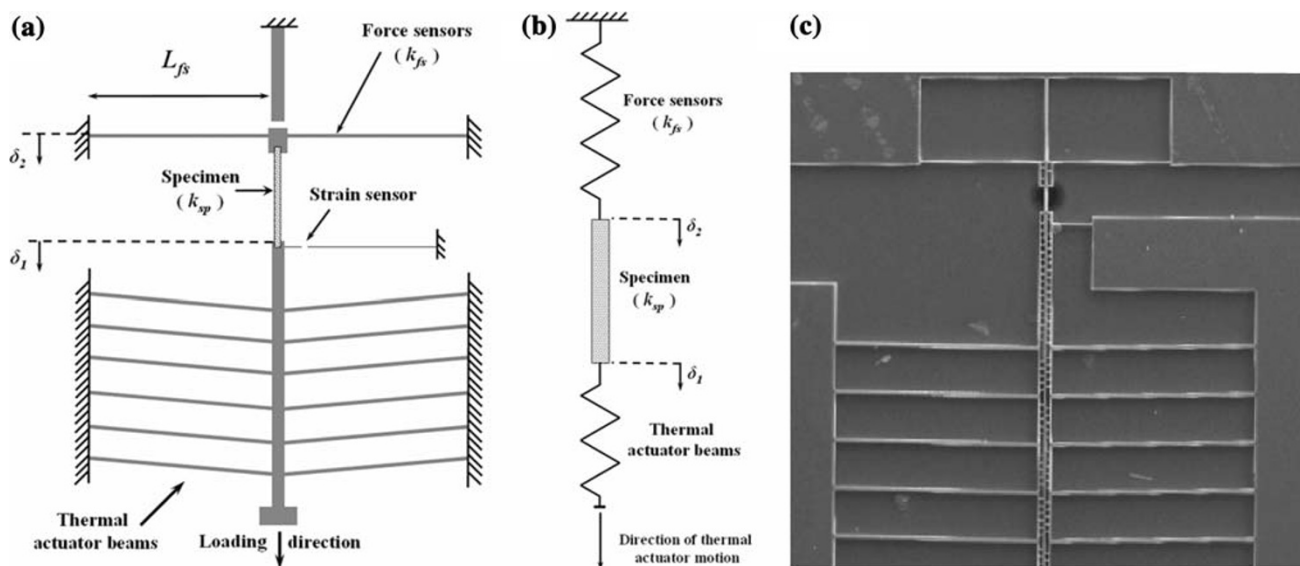

Fig. 1 a Schematic of the nanoscale uniaxial tensile testing device showing the thermal actuator and the integrated force and displacement sensing beams (not to *scale*). b Force equilibrium spring equivalent of the specimen-device system. c SEM image of the device
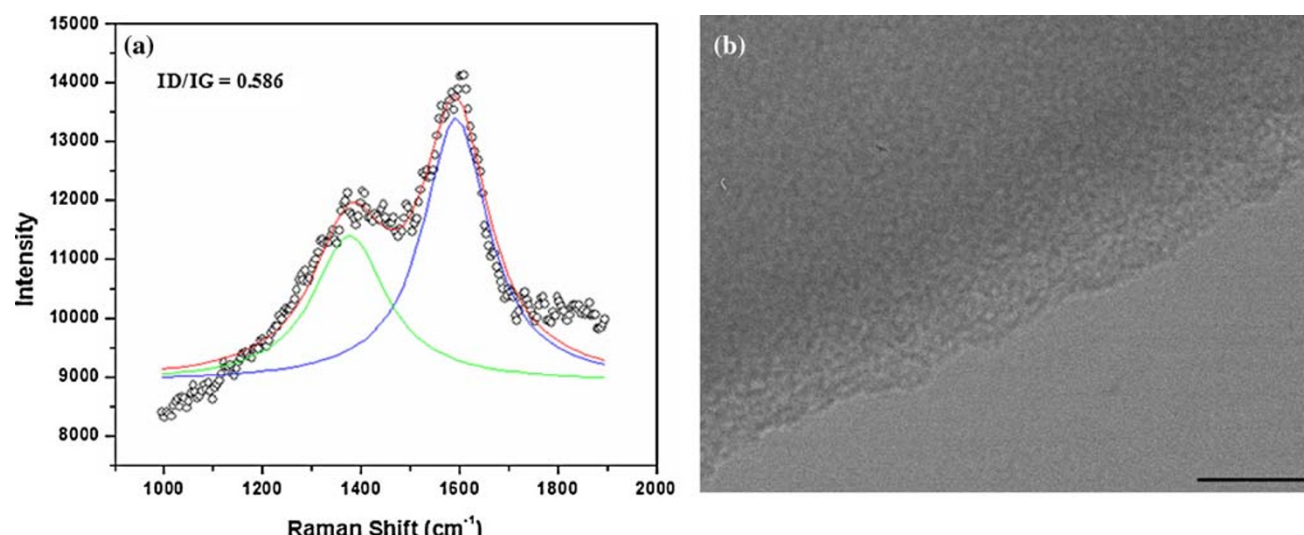
Fig. 2 a Raman spectra and **b** transmission electron micrograph for the freestanding glassy carbon film (*scale bar* is 20 nm)

flexural rigidity of the force sensing beam. The devices are first patterned using photolithography and then the silicon device layer is etched vertically with deep reactive ion etching. The microbeams are then released from the handle layer using hydro-fluoric acid vapor etching. Figure 1c shows scanning electron microscope (SEM) image of a fabricated device.

To achieve greater control over the length of the specimen that can be tested, specimens are fabricated separately from the device. The 4–6 nm-thick glassy carbon specimens used in this study were synthesized by pyrolyzing PFA precursor at 800 °C on a silicon substrate coated with a 500 nm-thick thermally grown silicon dioxide layer. Details of the synthesis and thickness characterization are given elsewhere [1, 8, 21]. We measured the Raman spectrum for a 5 nm-thick freestanding glassy carbon film to verify the structural characteristics of the carbon film. Figure 2 shows the experimental results, where the prominent peaks in the spectrum are the G peak at 1,580 cm^{-1} and D peak at 1,350 cm^{-1}, which confirms the formation of polyaromatic domains. In polyaromatic structures, the G peak represents the Raman-active E_{2g} in-plane vibration mode and the presence of disorder in the structure is indicated by the D peak, which represents the A_{1g} in-plane breathing mode [21]. The ratio of the intensity of these peaks, ID/IG, is called the relative peak intensity ratio and can be correlated to the reciprocal of the crystalline size along the basal plane, L_a, which was measured to be 7.5 nm.
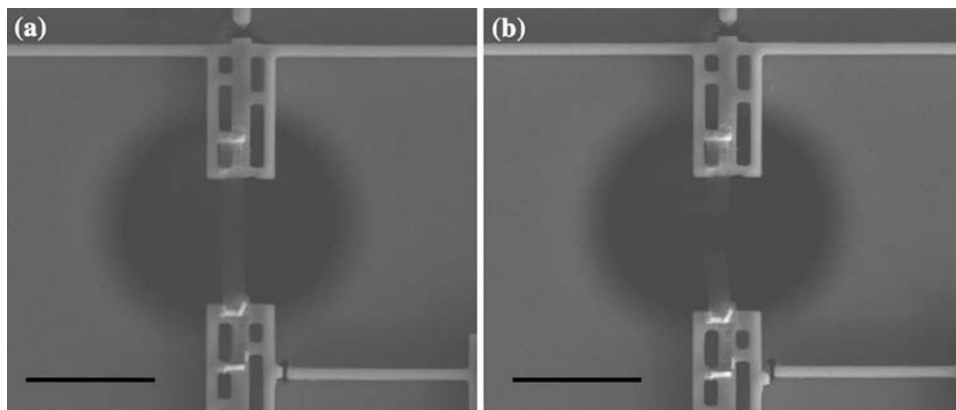
Tensile specimens, 100 microns long and 10 microns wide, were patterned using photolithography. The glassy carbon layer was then etched by oxygen plasma, which exposed the thermal oxide underneath. The oxide was then anisotropically etched with reactive ion etching. Next, the silicon substrate was isotropically etched using xenon

difluoride, resulting in freestanding bilayer beams of glassy carbon and oxide. An Omniprobe® nanomanipulator inside a dual gun focused ion beam—electron microscope with ion milling and platinum deposition capabilities is used to transfer and mount the bilayer on to the custom-designed micro-electro-mechanical tensile testing device. Hydrofluoric acid vapor etching was then used to remove the supporting silica layer, resulting in a freestanding ultrathin glassy carbon thin film securely attached to the device.

Experimental Results

Upon integration of the specimen, the device is wire bonded and placed inside the SEM with electrical feed-through for in situ testing inside the chamber. The specimens were loaded quasi-statically by applying a DC voltage across the thermal actuator beams. The device is equipped with sensors measuring displacements of the thermal actuator and the force sensing beams (δ_1 and δ_2, respectively, as shown in Fig. 1b). In each step of the voltage increment, these displacements were measured to obtain the force and elongation in the specimen using Eq. (1). The applied voltage was increased in small steps until the film fractured. Figure 3a shows the specimen mounted on the two mechanical jaws, bridging the thermal actuator and the force sensor beams. Figure 3b shows the specimen slightly curling up due to energy release after a brittle mode fracture. In situ testing in the SEM not only provides direct visual observation of the deformation in the specimen and more importantly at the specimen grips, but also enhances the resolution of the quantitative study. For example, SEM allows the thermal actuator and force sensor beam displacements to be measured with 50-nm resolution, which

Fig. 3 **a** SEM image of the freestanding ultrathin glassy carbon specimen mounted on the test device before loading. **b** The specimen after loading to fracture (*scale bar* is 50 μm)

results in 0.05% strain resolution for the 100 micron long specimens used in this study. The force resolution of the device would depend on the stiffness of the force sensing beam; for example, a beam 250 microns long (L_{fs}), 2 microns wide and 10 microns deep has a stiffness of 1.75 N/m, which results in 85 nN force and 1.75 MPa stress resolution for a nominally 5 nm-thick specimen. The stiffness of the force sensing beams is measured with a commercially calibrated spring structure, with the details described in [22]. The in situ SEM observations also enhance the consistency and repeatability of the experiments, and the maximum deviation of the data (from the spread of 5 experiments) is about 10% from the mean trend-line.

Figure 4 shows a representative stress–strain data for a 5 nm-thick freestanding glassy carbon specimen. The fracture mode is brittle and none of the specimens showed any sign of plasticity or necking. Also, none of the specimens showed slippage at the grips, hence no grip compliance correction was needed. The average Young's modulus for the five specimens was measured to be about 62 GPa, and the average tensile strength and strain values are
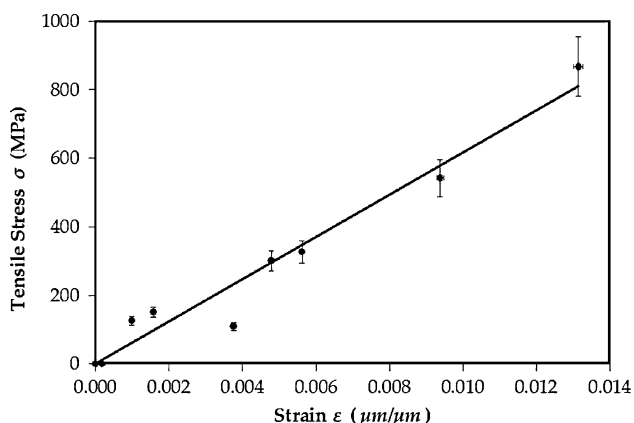

Fig. 4 Stress–strain diagram for a 5 nm-thick freestanding glassy carbon film

870 MPa and 1.3%, respectively. The corresponding values for bulk glassy carbon are about 30 GPa [23], 0.5–0.7% and 240 MPa, respectively [24], which show significant size effect on the stress-bearing capability of the material at the nanoscale, even though conventional elasticity theory is size independent. It is important to note that the oxide substrate does not influence the structure of the glassy carbon during the synthesis process [25].

Size Effect on Young's Modulus

We propose that the observed size effect can be explained by taking into consideration the effect of surface elastic properties on the mechanical properties of materials. Atoms at the surface have a lower coordination number (i.e. fewer neighboring atoms) than bulk atoms. Consequently, the nature of the chemical bond and the equilibrium interatomic distances are different at the surface compared to the bulk. This difference leads to surface stresses and surface energy [26], and therefore different mechanical properties for the surface and bulk material. As the length-scale of the material under study is reduced, the proportion of surface atoms to that of the bulk increases; and at the nanoscale, this ratio is large enough for surface properties to significantly affect the overall properties of the material. This surface effect can be accounted for by introducing the concept of surface elastic constant [27], S (units of *N/m*), which is a measure of the variation of surface stress (τ) with strain (ε). This can be expressed as [27, 28].

$$\tau_{\alpha\beta}(\varepsilon) = \tau_{\alpha\beta}(0) + S_{\alpha\beta}\varepsilon_\beta, \text{ i.e. } S_{\alpha\beta} = \left.\frac{\partial\tau_{\alpha\beta}}{\partial\varepsilon_\beta}\right|_{\varepsilon_\beta=0}$$

where $\alpha, \beta = 1 - 3$ (2)

At the nanoscale, the contributions from the surface elastic properties ($\tau_{\alpha\beta}$ and $S_{\alpha\beta}$) are significant and need to

be taken into account in addition to the bulk elastic properties. For the case of tensile loading, this can be expressed as [27]

$$E_{\text{nanoscale}} = E_{\text{bulk}} + 4\frac{S_{\alpha\beta}}{t} \qquad (3)$$

where $E_{\text{nanoscale}}$ is the measured Young's modulus, E_{bulk} is the modulus at the bulk scale and t is the critical size for the material under study, in this case, t being the thickness of the thin film. This equation illustrates the effect of length-scale of the material on the measured modulus value. However, glassy carbon is not crystalline as assumed in the above equations, and there is no reported value for the surface elastic constant for glassy carbon in the literature. We can approximate the surface elastic constant as $S = E_{\text{bulk}} \times r_0$, where r_0 is a characteristic length-scale representative of the material structure. Since glassy carbon does not have a long-range order in atomic arrangement, a representative length-scale can be determined by considering the misalignment of the polyaromatic domains in glassy carbon. It has been experimentally determined that the coherence length (atomic pair distribution function) of the domains in glassy carbon tapers off beyond a distance of about 1.2 nm [29]. Using $r_0 = 1.2$ nm and $E_{\text{bulk}} = 30$ GPa gives a surface elastic constant of 36 N/m and a modulus value of 59 GPa, which is close to the experimentally determined value of 62 GPa. Taking this consideration, we have plotted the variation of the modulus value for different values of S, using Eq. 3 (Fig. 5); the Young's modulus of glassy carbon at the bulk scale has been taken as 30 GPa. For surface elastic constant, $S = 40$ N/m, the modulus value ($E_{\text{nanoscale}}$) is very close to the experimentally obtained value of 62 GPa.
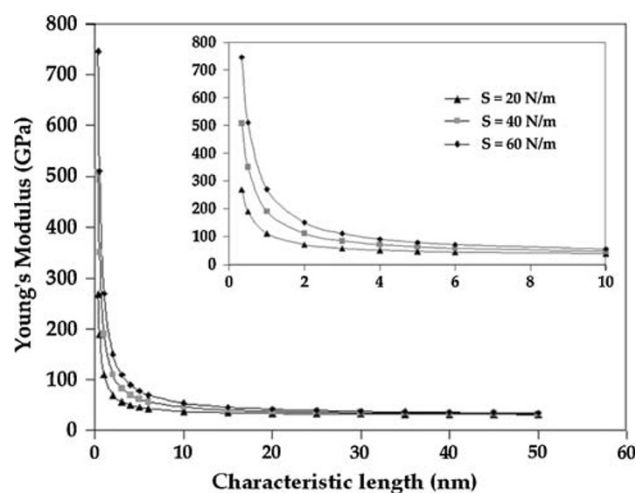
Conclusion

Glassy carbon is a nanoporous material that has superior thermal and chemical stability, which are attractive for applications in high temperature and corrosive environments. To study the effect of length-scale on the elastic properties of glassy carbon, we have synthesized films from PFA precursor pyrolyzed at 800 °C to obtain 4–6 nm-thick specimens. Using nanofabrication techniques, we integrated freestanding specimens with micro-electro-mechanical device to test the specimens in situ inside a SEM. The average values of the Young's modulus, fracture stress and strain of the thin film specimens were measured to be 62 GPa, 870 MPa and 1.3%, respectively. The size dependence of these elastic properties is explained with the effect of surface stress at this extreme length-scale. Efforts are currently being undertaken for in situ transmission electron microscope (TEM) testing to obtain direct visual evidence of any stress-based transformation.

Fig. 5 Effect of surface stresses on the Young's modulus value (based on Eq. 3); inset shows detailed view of the variation of modulus values for film thickness up to 10 nm

References

1. C.L. Burket, R. Rajagopalan, H.C. Foley, Overcoming the barrier to graphitization in a polymer-derived nanoporous carbon. Carbon **46**, 501–510 (2008)
2. R. Rajagopalan, A. Ponnaiyan, P.J. Mankidy, A.W. Brooks, B. Yi, H.C. Foley, Molecular sieving platinum nanoparticle catalysts kinetically frozen in nanoporous carbon. Chem. Commun. **21**, 2498–2499 (2004)
3. A. Merritt, R. Rajagopalan, H.C. Foley, High performance nanoporous carbon membranes for air separation. Carbon **45**, 1267–1278 (2007)
4. H.C. Foley, Carbogenic molecular sieves: Synthesis, properties and applications. Microporous Mater. **4**, 407–433 (1995)
5. C.J. Anderson, S.J. Pas, G. Arora, S.E. Kentish, A.J. Hill, S.I. Sandler, G.W. Stevens, Effect of pyrolysis temperature and operating temperature on the performance of nanoporous carbon membranes. J. Membr. Sci. **322**, 19–27 (2008)
6. R. Kostecki, X. Song, K. Kinoshita, Electrochemical analysis of carbon interdigitated microelectrodes. Electrochem. Solid-State Lett. **2**, 465–467 (1999)
7. C.L. Burket, R. Rajagopalan, A.P. Marencic, K. Dronvajjala, H.C. Foley, Genesis of porosity in polyfurfuryl alcohol derived nanoporous carbon. Carbon **44**, 2957–2963 (2006)
8. C.L. Burket, R. Rajagopalan, H.C. Foley, Synthesis of nanoporous carbon with pre-graphitic domains. Carbon **45**, 2307–2310 (2007)
9. W.V. Kotlensky, H.E. Martens, Tensile properties of glassy carbon to 2900 °C. Nature **206**, 1246–1247 (1965)
10. E. Fitzer, W. Schäfer, The effect of crosslinking on the formation of glasslike carbons from thermosetting resins. Carbon **8**, 353–364 (1970)

11. J.X. Zhao, R.C. Bradt, P.L. Walker Jr, The fracture toughness of glassy carbons at elevated temperatures. Carbon **23**, 15–18 (1985)
12. O.J.A. Schueller, S.T. Brittain, C. Marzolin, G.M. Whitesides, Fabrication and characterization of glassy carbon MEMS. Chem. Mater. **9**, 1399–1406 (1997)
13. B.A. Samuel, M.A. Haque, Y. Bo, R. Rajagopalan, H.C. Foley, Mechanical testing of pyrolysed poly-furfuryl alcohol nanofibres. Nanotechnology **18**, 115704 (8 pp) (2007)
14. C. Lee, X. Wei, J.W. Kysar, J. Hone, Measurement of the Elastic Properties and Intrinsic Strength of Monolayer Graphene. Science **321**, 385–388 (2008)
15. I.W. Frank, D.M. Tanenbaum, A.M. van der Zande, P.L. McEuen, Mechanical properties of suspended graphene sheets. J. Vac. Sci. Technol. B **25**, 2558–2561 (2007)
16. G.M. Pharr, A. Bolshakov, Understanding nanoindentation unloading curves. J. Mater. Res. **17**(10), 2660–2671 (2002)
17. M.R. VanLandingham, Review of instrumented indentation. J. Res. Natl. Inst. Stand. Technol **108**(4), 249–265 (2003)
18. G. Shafirstein et al., Error analysis in nanoindentation. *Proceedings of the 1994 Fall Meeting of MRS, Nov 28-Dec 2 1994, Boston, MA, USA: Materials Research Society, Pittsburgh, PA, USA,* 1995
19. T.W. Tombler, C. Zhou, L. Alexseyev, J. Kong, H. Dai, L. Liu, C.S. Jayanthi, M. Tang, S.-Y. Wu, Reversible electromechanical characteristics of carbon nanotubes under local-probe manipulation. Nature **405**, 769–772 (2000)
20. A.V. Desai, M.A. Haque, Sliding of zinc oxide nanowires on silicon substrate. Appl. Phys. Lett. **90**, 033102 (2007)
21. H. Lee, R. Rajagopalan, J. Robinson, C.G. Pantano, Processing and characterization of ultrathin carbon coatings on glass. ACS Appl. Mater. Interfaces **1**(4), 927–933 (2009)
22. M.A. Haque, M.T.A. Saif, Application of MEMS force sensors for in situ mechanical characterization of nano-scale thin films in SEM and TEM. Sens. Actuators A **97–98**, 239–245 (2002)
23. G.M. Jenkins, K. Kawamura, *Polymeric carbons—carbon fibre, glass and char* (Cambridge University Press, Cambridge, 1976)
24. R.E. Bullock, J.L. Kaae, Size effect on the strength of glassy carbon. J. Mater. Sci. **14**, 920–930 (1979)
25. H. Lee, R. Rajagopalan, J. Robinson, C.G. Pantano, Processing and characterization of ultrathin carbon coatings on glass. ACS Appl. Mater. Interfaces **1**, 927–933 (2009)
26. W. Haiss, Surface stress of clean and adsorbate-covered solids. Rep. Prog. Phys. **64**, 591–648 (2001)
27. R.E. Miller, V.B. Shenoy, Size-dependent elastic properties of nanosized structural elements. Nanotechnology **11**, 139–147 (2000)
28. V.B. Shenoy, Atomistic calculations of elastic properties of metallic fcc crystal surfaces. Phys. Rev. B **71**, 094104 (2005)
29. M.A. Smith, H.C. Foley, R.F. Lobo, A simple model describes the PDF of a non-graphitizing carbon. Carbon **42**, 2041–2048 (2004)